university of groningen

University Medical Center Groningen

University of Groningen

Temperature-induced magnetization reversal in a YVO3 single crystal

Ren, Y; Palstra, T.T.M.; Khomskii, D.I; Pellegrin, E.; Nugroho, A.A.; Menovsky, A.A.; Sawatzky, G.A

Published in:
Nature

DOI:
10.1038/24802

IMPORTANT NOTE: You are advised to consult the publisher's version (publisher's PDF) if you wish to cite from it. Please check the document version below.

Document Version
Publisher's PDF, also known as Version of record

Publication date:
1998

Link to publication in University of Groningen/UMCG research database

Citation for published version (APA):
Ren, Y., Palstra, T. T. M., Khomskii, D. I., Pellegrin, E., Nugroho, A. A., Menovsky, A. A., & Sawatzky, G. A. (1998). Temperature-induced magnetization reversal in a YVO3 single crystal. *Nature*, *396*(6710), 441 - 444. https://doi.org/10.1038/24802

Copyright
Other than for strictly personal use, it is not permitted to download or to forward/distribute the text or part of it without the consent of the author(s) and/or copyright holder(s), unless the work is under an open content license (like Creative Commons).

The publication may also be distributed here under the terms of Article 25fa of the Dutch Copyright Act, indicated by the “Taverne” license. More information can be found on the University of Groningen website: https://www.rug.nl/library/open-access/self-archiving-pure/taverne-amendment.

Take-down policy
If you believe that this document breaches copyright please contact us providing details, and we will remove access to the work immediately and investigate your claim.

Downloaded from the University of Groningen/UMCG research database (Pure): http://www.rug.nl/research/portal. For technical reasons the number of authors shown on this cover page is limited to 10 maximum.

Download date: 23-08-2022

field lines are puzzling, however. In principle, the plasma should fall freely along such lines, reaching speeds of 50 km s^{-1} or more, but that conflicts with the speeds in fact seen (a few kilometres per second). A somewhat similar situation prevails in spicules, also without a satisfactory explanation.

Why has counter-streaming not been detected in previous Doppler observations of filaments? We made Dopplergrams from pairs of red-wing and blue-wing images, as have many other authors[4–14]. We concluded that our line-of-sight velocity maps alone do not reveal counter-streaming because a simple subtraction of moderate-resolution images, taken in opposite wings, will usually result in a null Doppler signal. Second, motions of the chromospheric background can corrupt the signal in the filament, unless spatial resolution is sufficiently high. Last, isolated pairs of images do not reveal the long distances traversed by the moving knots of mass.

Detection of the counter-streaming requires high spatial resolution, a favourable filament orientation, time-series of observations in both wings simultaneously over several hours, carefully registered images and a high rate of image projection. The filament we observed is quite typical. We therefore suggest that counter-streaming is a feature common to all quiescent filaments.

Our observations contradict all contemporary prominence models, even those of barbs, as these models do not allow any vertical motions, let alone counter-streaming. Simply allowing horizontal field lines to drift up and down, while carrying blobs of mass, will not easily explain counter-streaming, for then alternate field lines would have to pass each other and travel long diagonal distances. Such complex motions seem unrealistic to us.

We propose instead a conceptual model[18] in which field lines bend down from the spine to the chromosphere (see Fig. 2 centre). In this model, the mass flows along the field lines: it is not carried by moving horizontal field lines, and does not cross the field lines. The tension of such steeply inclined field lines, which are embedded in the prominence sheet, might act to restrain the prominence from erupting. Certainly the existence of such field lines needs to be incorporated in any acceptable model of prominence eruption. □

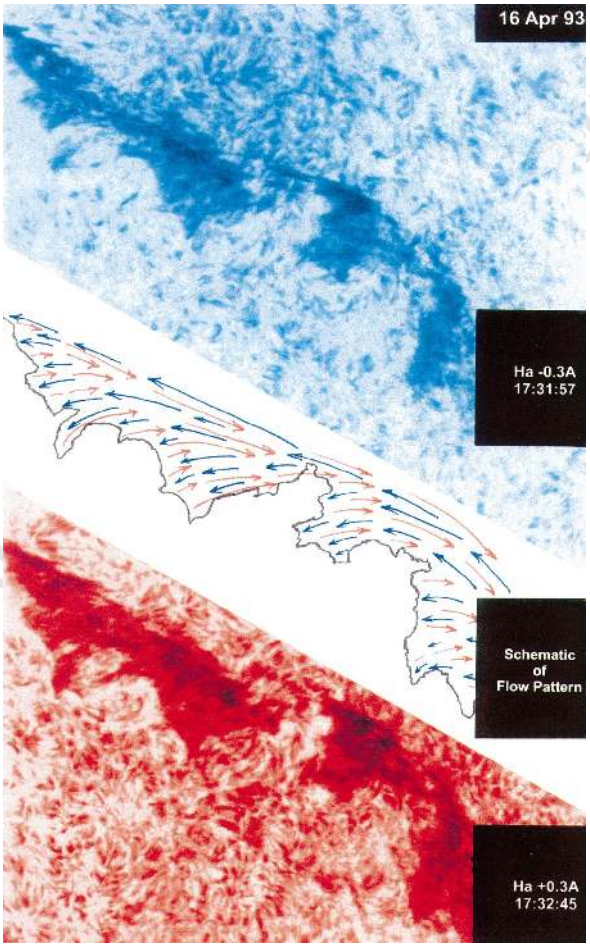

Figure 2 Images on 16 April, showing the inclined threads. In the blue wing, the streaming is only westward along the spine and downward into the barbs on the near side of the filament (blue arrows in the middle panel). In the red wing, the streaming is only eastward along the spine and up in the same barbs on the near side (red arrows in middle panel). This systematic pattern appears most clearly on 16 April, when the filament lay just inside the east limb. Finally, on April 20, when the filament had crossed the central meridian, the pattern reverses, with a predominant eastward streaming in the blue wing although both eastward and westward streaming are seen in different filament threads.

Received 24 April; accepted 10 September 1998.

1. Jackson, B. V. & Howard, R. CME mass distribution derived from SOLWIND coronagraph observations. *Sol. Phys.* **148,** 359–370 (1993).
2. Priest, E., McKay, D. & Longbottom, A. Dipped magnetic field configuration associated with filaments and barbs. *Astron. Astrophys* (in the press).
3. Aulanier, G., Demoulin, P., van Driel-Gesztely, L., Mein, P. & DeForest, C. 3-D magnetic configurations supporting prominences II. *Astron. Astrophys* **335,** 309–322 (1998).
4. Dunn, R. B. *A Photometric Investigation of the Solar Chromosphere.* Thesis, Harvard Univ. (1960).
5. Engvold, O. The small-scale velocity field of a quiescent prominence. *Sol. Phys.* **70,** 315 (1981).
6. Engvold, O. in *New Perspectives on Solar Prominences* (eds Webb, D., Rust, D. m. & Schmeider, B.) (IAU Colloq. 167, Kluwer Academic Press, in the press).
7. Engvold, O. The fine structure of prominences I. *Sol. Phys.* **49,** 283–295 (1976).
8. Liggett, M. & Zirin, H. Rotation in prominences. *Sol. Phys.* **91,** 259–267 (1984).
9. Mein, P. in *Solar Coronal Structures* (eds Rusin, V., Heinzel, P. & Vial, J. C.) 289–296 (IAU Colloq. 144, Veda Publishing House, 1993).
10. Martres, M. J., Mein, P., Schmeider, B. & Soru-Escaut, I. Structure and evolution in quiescent prominences. *Sol. Phys.* **69,** 301–312 (1981).
11. Mahlerbe, J., Schmeider, B. & Mein, P. Dynamics in the filaments. *Astron. Astrophys.* **102,** 124–128 (1981).
12. Mahlerbe, J. M., Schmeider, B., Ribes, E. & Mein, P. Mass motions in filaments. *Astron. Astrophys.* **119,** 197–206 (1983).
13. Engvold, O. & Keil, S. L. in *Coronal and Prominence Plasmas* (ed. Poland, A. I.) (NASA Conf. Publ. 2442, NASA, Washington, DC, 1986).
14. Kubota, J. & Uesegi, A. Vertical motion of a prominence. *Publ. Astron. Soc. Jpn* **38,** 903–909 (1986).
15. Leroy, J.-L., Bommier, V. & Sahal-Brechot, S. New data on the magnetic structure of quiescent prominences. *Astron. Astrophys.* **131,** 33–44 (1984).
16. Hundhausen, J. R. & Low, B. C. Magnetostatic structure of the solar corona 2, the magnetic topology of quiescent prominences. *Astrophys. J.* **443,** 818–832 (1995).
17. Bothmer, V. & Schwenn, R. Eruptive prominences as sources of magnetic clouds in the solar wind. *Space Sci. Rev.* **70,** 215–220 (1994).
18. Martin, S. F. & Echols, C. R. in *Solar Surface Magnetism* (eds Rutten, R. J. & Schrijver, C. J.) 339–346 (Kluwer Academic, Dordrecht, 1994).

Acknowledgements. We thank H. Zirin for the observing run at BBSO, D. Martin for reproducing the original photographic data in digital movie format, and R. Ewald for her assistance in preparing the illustrations.

Correspondence and requests for materials should be addressed to J.B.Z. (e-mail: jzirker@noao.edu).

Temperature-induced magnetization reversal in a YVO_3 single crystal

Y. Ren*, T. T. M. Palstra†, D. I. Khomskii*, E. Pellegrin*, A. A. Nugroho‡§, A. A. Menovsky‡ & G. A. Sawatzky*

** Solid State Physics Laboratory, † Inorganic Solid State Chemistry Laboratory, Materials Science Centre, University of Groningen, Nijenborgh 4, 9747 AG Groningen, The Netherlands*
‡ Van der Waals-Zeeman Institute, University of Amsterdam, Valckenierstaart 65, 1018 XE Amsterdam, The Netherlands

The total energy of a magnet in a magnetic field is lowest when the magnetic moment is aligned parallel to the magnetic field. Once aligned, the magnetic moment can be reversed by applying a sufficiently large field in the opposite direction. These properties form the basis of most magnetic recording and storage devices. But the phenomenon of magnetization reversal in response to a change in temperature (in a small magnetic field) is rarer. This effect occurs in some ferrimagnetic materials consisting of two or

§ Jurusan Fisika, Fakultas Matematika dan Ilmu Pengetahuan Alam, Institut Teknologi Bandung, Indonesia.

Nature © Macmillan Publishers Ltd 1998

more types of antiferromagnetically ordered magnetic ions[1], and forms the operational basis of ferrimagnetic insulators. Here we report the observation of multiple temperature-induced magnetization reversals in YVO_3. The net magnetic moment is caused by a tilting of the antiferromagnetically aligned moments of (crystallographically identical) V^{3+} ions, due to orthorhombic distortion in the crystal structure. We observe an abrupt switching at 77 K associated with a first-order structural phase transition, and a gradual reversal at ~95 K without an accompanying structural change. The magnetization always reverses if the crystal is cooled or warmed through these two temperatures in modest fields. We propose a possible mechanism involving a change in orbital ordering which may be generic to a broad class of transition metal oxides.

Transition metal oxides with the perovskite structure display a large variety of properties such as high-temperature superconductivity, colossal magnetoresistance[2,3] and very diverse magnetic properties. We now report on another novel and peculiar phenomenon in YVO_3: multiple and reversible sign changes in the magnetization with temperature. Such magnetic-moment reversals have been observed in those ferrimagnets[1] with strong magnetic anisotropy that exhibit a compensation temperature. The net magnetization, initially oriented parallel to the field, changes sign at this temperature and the metastable, energetically unfavourable state is fixed by the strong anisotropy. For such an effect to occur, inequivalent sites must exist. In YVO_3, however, all magnetic V sites are equivalent, as shown by the crystallographic data.

Close to our situation is the observation of a 'diamagnetic' response in $LaVO_3$ (refs 4–6). Upon weak-field cooling, this system exhibits a magnetization opposite to the applied magnetic field below a structural phase transition temperature $T_t = 138\,K < T_N = 142\,K$, where T_N is the magnetic ordering (Néel) temperature. It has been suggested that this diamagnetic response is due to a reversal of a canted-spin moment on traversing the first-order Jahn–Teller phase transition at T_t, below which the orbital angular momentum is maximized[6–8], and that the response of the orbital moment to the forces generated at the first-order phase transition can reverse the Dzyaloshinsky vector so as to create a canted spin in a direction opposite to the applied field, given that T_t is close to T_N. Other polycrystalline samples of V^{3+} perovskites show weak indications of anomalous behaviour[7–9]. We demonstrate the dramatic behaviour of single crystals of YVO_3 in which multiple magnetization switching is clearly observed. In contrast with $LaVO_3$, YVO_3 provides a wide temperature window between T_N and the first-order phase transition which we refer to as T_s, enabling us to study the effect in detail. Furthermore, an additional magnetization reversal is observed, irrespective of the cooling conditions.

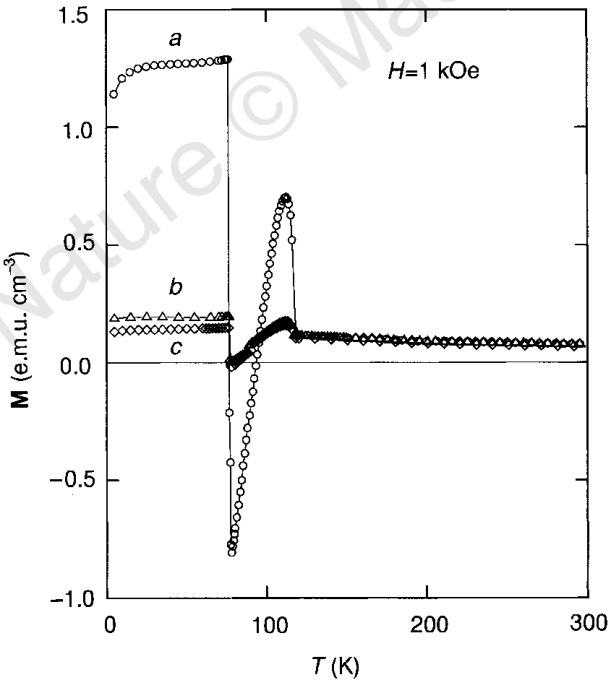

Figure 1 Temperature dependence of the magnetization in an applied magnetic field of 1 kOe along the *a*-, *b*- and *c*-axes, respectively. Upon cooling the sample in a fixed magnetic field $H < 4$ kOe below $T_N = 116$ K, the magnetization after first increasing starts decreasing and crosses zero at $T^* \approx 95$ K to a large negative value. With further cooling, it jumps at $T_s = 77$ K to a large positive value. This second transition exhibits hysteresis that is consistent with a first-order transition, as inferred from the structural data. In contrast with $LaVO_3$, we observe not only an abrupt magnetization reversal at the first-order transition T_t, but also a gradual reversal near 95 K.

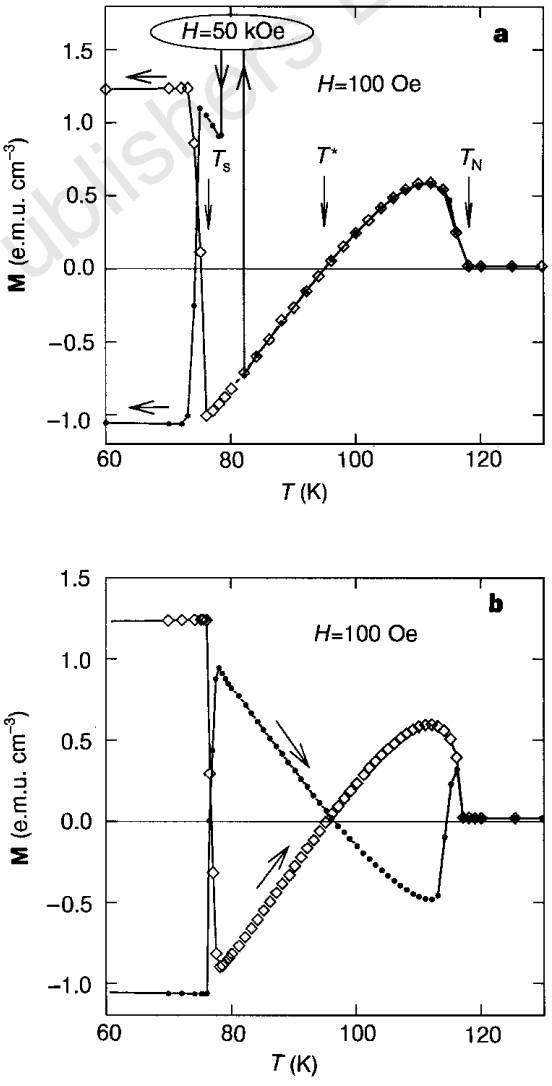

Figure 2 Magnetization versus temperature in a field of 100 Oe, demonstrating the memory effect upon the application of large fields. In the curve marked by filled circles in **a** we follow **M** with decreasing temperature down to a temperature below T^*; a high field is then applied to flip the magnetization positive, after which the field is lowered again to 100 Oe and the temperature decreases. The curve marked by diamonds is measured without intermediate application of the high field. In **b**, we show the curves with increasing temperature starting from below T_s: the curve marked by diamonds without having 'trained' the sample, and the curve marked by filled circles after 'training' as described for **a**. This demonstrates the reversibility: upon warming, **M** now switches from negative below T_s, to positive for $T_s < T < T^*$, and becomes negative for $T > T^*$. it is thus nearly a 'mirror image' of the behaviour shown in Fig. 1 and the diamond marked curve in **b**, except that it becomes positive again close to T_N.

Nature © Macmillan Publishers Ltd 1998

YVO_3 has a distorted perovskite structure of the type $GdFeO_3$ (crystal symmetry *Pbnm*) at all temperatures. It has two magnetic phases: one at $T_s \approx 77\,K < T < T_N = 116\,K$ and another at $T < T_s$. The detailed magnetic structure of these phases is controversial[10,11] but is not crucial for the experimental observations reported here.

The distorted crystal structure naturally leads to canted spin structures. As the oxygen ions mediating the superexchange interaction between the two nearest neighbour V ions are not at an inversion centre, the antisymmetric Dzyaloshinsky–Moriya (DM) interaction of the form $\mathbf{D}\cdot(\mathbf{S}_1 \times \mathbf{S}_2)$ will be present, where $\mathbf{D}$ is the so-called Dzyaloshinsky vector and $\mathbf{S}_1$ ($\mathbf{S}_2$) are the V spins corresponding to the two magnetic sublattices. The DM interaction, which prefers canted spin arrangements, is in competition with the quite different ordinary Heisenberg exchange $J\mathbf{S}_1\cdot\mathbf{S}_2$, which prefers collinear spin arrangements. Also, because the oxygen octahedra coordinating the V ions are twisted to form a staggered V–O bond direction along the *c*-axis, the single-ion anisotropy easy axis is staggered. Both of these mechanisms can lead to weak ferromagnetism[12]. The fact that YVO_3 is a weak ferromagnet with spin canting has been established from measurements on powder samples[13]. Several batches of crystallographically pure large single crystals ($5 \times 5 \times 5\,mm^3$) were grown by the floating-zone method. The magnetic measurements made on a large number of our single crystals all reveal the same unusual behaviour, with several magnetization reversals upon cooling in a weak magnetic field (Fig. 1).

Even more striking, is the observation of a memory effect shown in Fig. 2a. This indicates that the sign of the magnetization can be reversed by the application of a large enough field, but that upon lowering the field, the temperature-dependent net magnetic moment $\mathbf{M}(T)$ always changes sign, irrespective of what its sign was, when crossing T_s both on cooling and warming. The same is also true for the second crossing at T^*.

Although we do not as yet have a detailed microscopic theory for the magnetization reversal with temperature, we propose the model shown in Fig. 3. As mentioned above, there are two mechanisms for producing a canted spin structure in these materials: single-ion magnetic anisotropy and DM coupling. These two canting mechanisms produce the net moment in the *a*–*c* plane, and in our model we assume that they are oriented in opposite directions. We checked that the observed phenomena are connected to spin canting: the differential susceptibility $d\mathbf{M}/dH$ is always positive (even in the 'diamagnetic' state) and the net moment is ~0.01 Bohr magneton per V ion, which for an $S = 1$ system corresponds to a canting angle of ~0.2°.

Using this model, we present in Fig. 3 a pictorial view of what could happen as a function of temperature. We start at temperatures just below T_N (Fig. 3a). Here, the two sublattice spins prefer to lie close to a local easy axis if the local magnetic anisotropy is large, resulting in a net magnetic moment, as shown. As T decreases, this net moment will first grow because of the development of a sublattice magnetization due to superexchange. However, as the sublattice magnetization develops, so does the DM coupling, which tends to cant the spins in the opposite direction. Consequently, the net moment will reach a maximum and then decrease. It crosses zero at the temperature below which the DM interaction dominates. This will result in a moment opposite to the small applied field. It could only reverse to its lowest energy state in the field by reversing the two sublattices on a macroscopic scale, resulting in a frozen in metastable state (Fig. 3b). A large external magnetic field can overcome the barrier for rotation of the sublattice spins, resulting in a reversal of the sublattice spin orientation (Fig. 3c). The net moment is now oriented parallel to the field and will remain so upon lowering the field. If we now increase the temperature, we return to the situation where magnetic anisotropy dominates. Thus, the net moment will change sign again, now turning negative for $T > 95\,K$ (the curve marked by filled circles in Figs 2b, 3d). Once we get close enough to T_N, the energy barrier for the reversal of the sublattice magnetization will eventually become very small. Any finite field will flip the net moment again to a positive value and reach a maximum just below T_N, dropping to zero at T_N (Fig. 2). This model explains all the data from high temperatures down to the first-order phase transition at 77 K.

The magnetization reversal at T_s remains more of a puzzle. It follows from our results that the ferromagnetic moment is oriented along the *a*-axis both above and below T_s. From neutron scattering, we know that the magnetic structure changes at T_s from *C*- to *G*-type, as proposed by Kawano *et al.*[11] This is definitely connected with a change of orbital ordering occurring at T_s. Low-temperature single-crystal X-ray diffraction (Y.R. *et al.*, unpublished results) of YVO_3 shows that, whereas above T_s the V–O bond lengths are almost equal, the first-order phase transition is accompanied by a strong distortion of these bond lengths, resulting in pairs of long (2.052 Å), intermediate (1.992 Å) and short (1.975 Å) V–O bonds. The long and short bonds are oriented alternately along the [110] and [1$\bar{1}$0] in the basal *a*–*b* plane, whereas the intermediate one of 1.992 Å is along the *c*-axis, similar to the structure of $LaMnO_3$; such a distortion corresponds to orbital ordering, with the d_{xy}

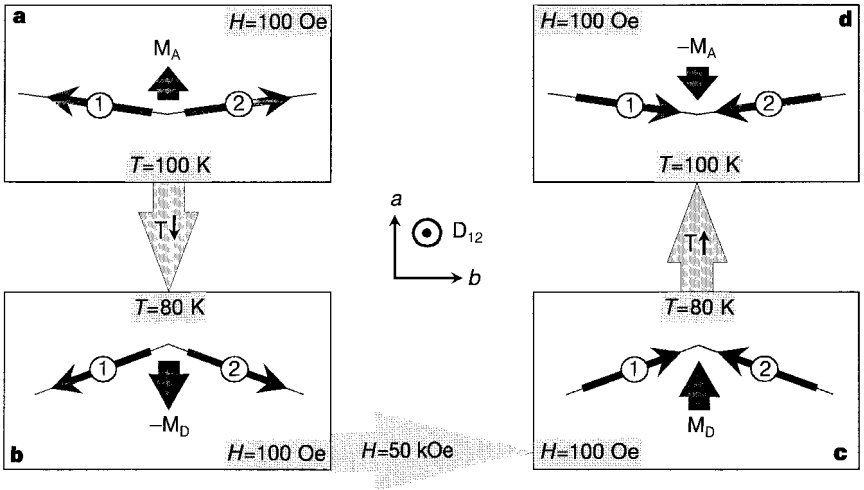

Figure 3 Pictorial view of the temperature dependence of the magnetization. **a**, Just below T_N, the two sublattice spins prefer to lie close to a local easy axis if the local magnetic anisotropy is large, resulting in a net magnetic moment parallel to the applied field. **b**, As T decreases below $T^* = 95\,K$, the DM interaction dominates which tends to cant the spins in opposite direction. A large external magnetic field can overcome the barrier for rotation of the sublattice spins, resulting in a reversal of the sublattice spin orientation. **c**, The net moment is now oriented parallel to the field and will remain so upon lowering the field. If we now increase the temperature, we come back to the situation where the magnetic anisotropy dominates. **d**, Thus, the net moment will change sign again, turning negative for $T > 95\,K$.

Nature © Macmillan Publishers Ltd 1998

Nature © Macmillan Publishers Ltd 1998

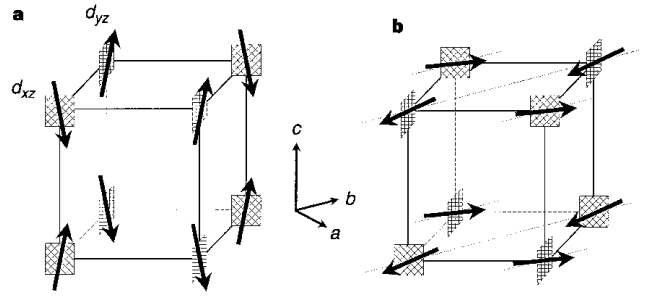

Figure 4 Suggested orbital ordering below and above $T_s = 77$ K. **a**, A *C*-type orbital ordering with a *G*-type spin ordering; and **b**, a *G*-type orbital ordering with a *C*-type spin ordering. The dotted lines are along the *b*-axis. The hatched squares indicate the planes in which the occupied *d* orbitals lie. The d_{xy} orbitals that are in each case occupied by one electron are omitted for clarity.

orbital occupied at each V^{3+} site and the second electron occupying, respectively, the d_{xz} and d_{yz} orbitals in two sublattices as shown in Fig. 4. According to the Goodenough–Kanamori rules[14], this orbital occupation naturally leads to the *G*-type antiferromagnetism[11]. A similar result was also obtained by band-structure calculation[15]. From Fig. 1, we see that the ferromagnetic component is both above and below T_s oriented parallel to the *a*-axis of the crystal; the magnetic structure above T_s must therefore be of *C*-type. Then, according to Bertaut's symmetry considerations[12], the easy axis below T_s should be close to the *c* direction in order for the weak moment to remain along *a*. From this, we conclude that the easy axis must indeed change on going through the phase transition. The *C*-type magnetic ordering observed between T_s and T_N (ref. 11) should then correspond to an orbital structure, with the alternation of the sublattices also being along the *c* direction and, as discussed above, with the easy axis almost parallel to *b*. Such a drastic change of the magnetic properties at T_s can lead to a change in the relative role of the DM interaction and the anisotropy. Careful neutron scattering experiments are needed to clarify the behaviour of YVO_3 across T_s.

Our results make it difficult to compare $LaVO_3$ and YVO_3 in detail: single crystals of $LaVO_3$ are needed, although the close proximity of T_N and T_t in $LaVO_3$ will be a complicating factor. □

Received 19 June; accepted 19 August 1998.

1. Menyuk, N., Dwight, K. & Wickham, D. G. Magnetisation reversal and asymmetry in cobalt vanadate (IV). *Phys. Rev. Lett.* **4,** 119–120 (1960).
2. Goodenough, J. B. Metallic oxides. *Prog. Solid State Chem.* **5,** 145–399 (1973).
3. Khomskii, D. I. & Sawatzky, G. A. Interplay between spin, charge and orbital degrees of freedom in magnetic oxides. *Solid State Commun.* **102,** 87–99 (1997).
4. Shirakawa, N. & Ishikawa, M. Anomalous diamagnetism of a peroviskite $LaVO_3$. *Jpn Appl. Phys.* **30,** L755–L756 (1991).
5. Mahajan, A. V., Johnston, D. C., Torgeson, D. R. & Borsa, F. Magnetic properties of $LaVO_3$. *Phys. Rev. B* **46,** 10966–10972 (1992).
6. Goodenough, J. B. & Nguyen, H. C. The peculiar ferromagnetism of $LaVO_3$. *C.R. Acad. Sci., Paris* **319,** 1285–1291 (1994).
7. Nguyen, H. C. & Goodenough, J. B. Magnetic studies of some orthovanadates. *Phys. Rev. B* **52,** 324–334 (1995).
8. Nguyen, H. & Goodenough, J. B. Magnetic and transport properties of $CeVO_3$. *J. Solid State Chem.* **119,** 24–35 (1995).
9. Corti, M., Cintolesi, A., Lascialfari, A., Rigamonti, A. & Rossetti, G. Magnetic properties of YVO_3 from susceptibility and ^{89}Y NMR measurements. *J. Appl. Phys.* **81,** 5286–5288 (1997).
10. Zubkov, V. G., Bazuev, G. V. & Shveikin, G. P. Low-temperature neutron- and X-ray-diffraction investigations of rare-earth orthovanadites. *Sov. Phys. Solid State* **18,** 1165–1166 (1976).
11. Kawano, H., Yoshizawa, H. & Ueda, Y. Magnetic behavior of a Mott-insulator YVO_3. *J. Phys. Soc. Jpn* **63,** 2857–2861 (1995).
12. Bertaut, E. F. in *Magnetism* Vol. III (eds Rado, G. T. & Suhl, H.) 86–126 (Academic, New York and London, 1963).
13. Borukhovich, A. S., Bazuev, G. V. & Shveikin, G. P. Anomalies of the specific heat and magnetic thermodynamic parameters of yttrium orthovanadite. *Sov. Phys. Solid State* **16,** 191–192 (1974).
14. Goodenough, J. B. *Magnetism and the Chemical bond* (Interscience, New York–London, 1963).
15. Sawada, H., Hamada, N., Terakura, K. & Asada, T. Orbital and spin orderings in YVO_3 and $LaVO_3$ in the general gradient approximation. *Phys. Rev. B* **53,** 12742–12749 (1996).

Acknowledgements. We thank J. B. Goodenough for discussion of the results and for explaining his ideas on the origin of the magnetization reversal in $LaVO_3$; we also thank J. Rodriquez-Carvajal and E. F. Bertaut for discussion. This work is supported by the Netherlands Foundation for the Fundamental Research of Matter (FOM) and the Dutch Organization for the Advancement of Pure Research (NWO), and in part by EU (OXSEN).

Correspondence and requests for materials should be addressed to G.A.S.

Spontaneous ordering of bimodal ensembles of nanoscopic gold clusters

C. J. Kiely*, J. Fink*†, M. Brust†, D. Bethell† & D. J. Schiffrin†

** Materials Science and Engineering, Department of Engineering, The University of Liverpool, Liverpool L69 3BX, UK*
† Department of Chemistry, The University of Liverpool, Liverpool L69 7ZD, UK

The controlled fabrication of very small structures at scales beyond the current limits of lithographic techniques is a technological goal of great practical and fundamental interest. Important progress has been made over the past few years in the preparation of ordered ensembles of metal and semiconductor nanocrystals[1–7]. For example, monodisperse fractions of thiol-stabilized gold nanoparticles[8] have been crystallized into two- and three-dimensional superlattices[5]. Metal particles stabilized by

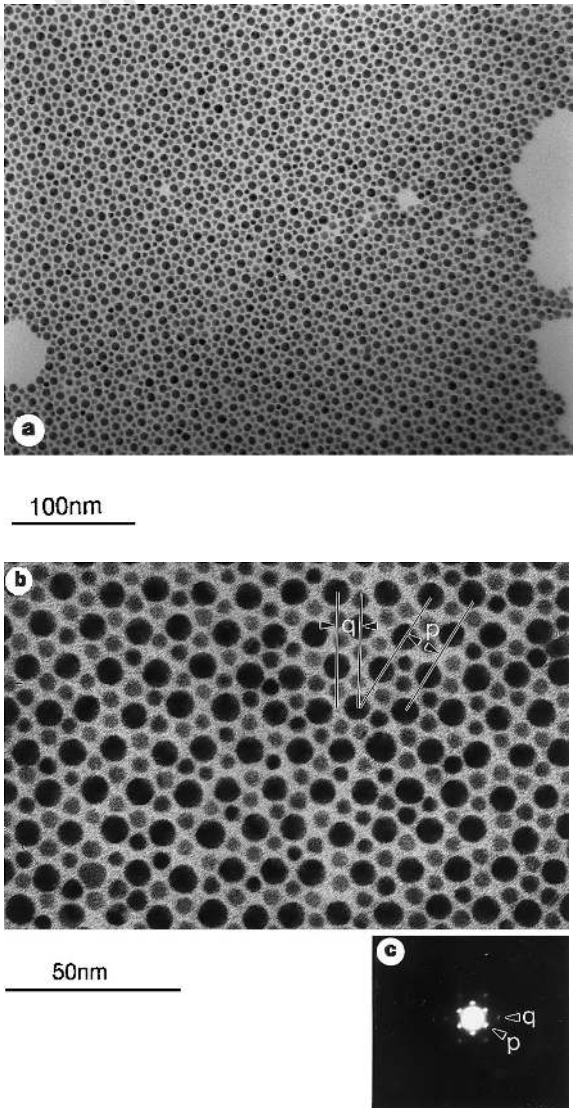

Figure 1 An ordered raft comprising Au nanoparticles of two distinct sizes with $R_B/R_A \approx 0.58$. Shown are electron micrographs at low (**a**) and higher (**b**) magnification. **c**, The low-angle superlattice electron diffraction pattern obtained from this bimodal raft structure.

Nature © Macmillan Publishers Ltd 1998